Orbital
The electronic journal of chemistry

the electronic journal of chemistry

Full Paper | http://dx.doi.org/10.17807/orbital.v13i2.1488

Mechanochemical Synthesis of Expanded Vermiculite with Urea for Filler into Alginate/Collagen Spherical Capsules: A Urea Slow-release System

Douglas Santos de Oliveira, Silvia Jaerger, and Rafael Marangoni*

The annual growth of the world population increasingly provokes the search for highly productive agriculture, with an effective and economical application of fertilizers capable of supplying the necessary nutrients to the plants. In this context, the development of technologies to control these fertilizers in the environment is relevant. This study presents a potential slow-release fertilizer created from the intercalation of urea in the expanded vermiculite (EV) and encapsulated in a sphere constituted of alginate/collagen. The intercalation tests were performed by the mechanochemical process between EV and urea, and the intercalated materials were characterized by XRD, TGA/DSC, and FTIR. The results showed that urea was intercalated at all studied ratios, but the sample containing 20% of urea (EVU20%) did not present peaks from the starting reagents. Thus, the sample EVU20% was chosen for the encapsulation process and release test. Urea concentration released was determined by colorimetric analysis, and the test revealed that the spheres produced with EVU20% encapsulated into an alginate/collagen matrix were able to release the urea up to 210 hours. Therefore, this system has the potential to be a new fertilizer of slow-release to be applied in agriculture, promoting the gradual release of urea for plant development.

Graphical abstract

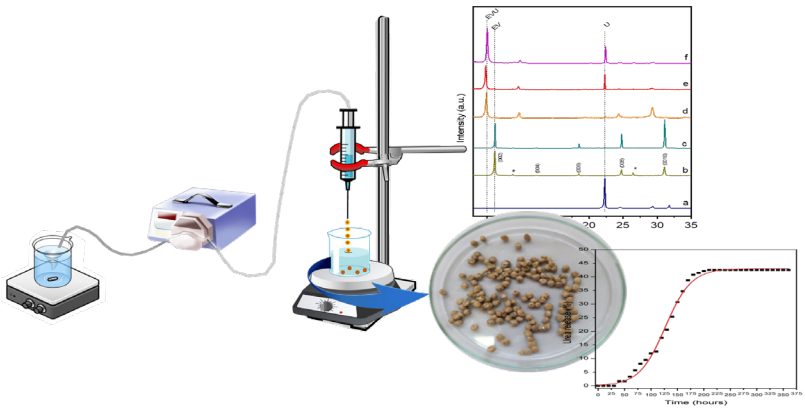

Keywords

Fertilizer
Mechanochemical process
Slow-release
Urea
Vermiculite

Article history

Received 31 March 2020
Revised 11 July 2020
Accepted 05 July 2021
Available online 20 June 2021

Handling Editor: Sergio R. Lázaro

1. Introduction

Currently, the world agricultural sector is looking for new management alternatives to optimize and enhance its production. New technologies are in development, where, among them, new technologies are the improvement of new fertilizers [1].

Commercial fertilizers applied to the soil may offer

Laboratório de Tecnologia e Química de Materiais Avançados (TEQMA), Departamento de Química, Universidade Estadual do Centro-Oeste – UNICENTRO/CEDETEG, Rua Alameda Élio Antônio Dalla Vecchia, 838 – CEP 85040–167 – Bairro Vila Carli, Guarapuava – Paraná, Brazil. *Corresponding author. E-mail: **rmarangoni@unicentro.br**

problems due to their short durability with the climatic variation. Therefore, the investigation and study of new applications to allow the complete development of plants are desirable. The importance of improving a higher quality fertilizer is to ensure that it can withstand the two primary weather conditions, which are the leaching induced by rain and volatilization caused by the sun [2].

Enhanced fertilizers, also known as "smart" fertilizers, have two application classes: slow-release fertilizers and controlled-release fertilizers [3]. The first class is characterized by the dependence on climatic factors, and the total release time is not predicted. The second class is necessarily known for the release time and stipulates the release time interval [4].

Another critical factor in the development of these fertilizers is the use of cost-effective coating materials. Many researchers are working on cellulosic and polymeric materials, such as the study by Elhassani et al., 2019, which coated urea with lignocellulosic derivatives and mesoporous hydroxyapatite, achieving this slow-release fertilizer's durability within 60 days [5].

Kanawy et al. (2019) have investigated the application of acrylic acid, 2-hydroxyethyl methacrylate, and montmorillonite in sodium alginate to create a polymeric structure for urea Methylenebisacrylamide and potassium persulphate were also used as crosslinkers as an indicator in aqueous solution (this sentence is a bit confused). The results showed that the amount of released urea increased as a function of montmorillonite concentration [6].

Thus, these recently published works, among others that encompass the same theme [7, 8], becomes understandable there is a need to invest in advanced fertilizer research. By the way, an alternative in producing a slow-release fertilizer is to use clay minerals capable of being a host to sources of N, P, and K, which are then covered by a biodegradable polymer matrix.

The two most essential steps in manufacturing the slow-release fertilizer are the intercalating process and the polymeric coating that this material receives. It is necessary to know each material's structural characteristics to choose the intercalation method and the polymeric materials suitable for encapsulation. For the intercalation step of this study, the mechanochemical method was chosen to intercalate urea (U) into the interlayer space of the expanded vermiculite (EV) (the clay mineral selected for this study) [9]. Moreover, after obtained the new material composed of the EV and Urea, it is possible to coat them with a biodegradable polymeric matrix. As mentioned, the encapsulation step is essential to guarantee a gradual release of the coated material; The most used techniques for the manufacture of polymeric encapsulations are evaporation, spray-drying, and phase separation (coacervation). The phase separation technique is the most used for the manufacture of slow-release fertilizer and drugs, passing through the phase separation phase of the polymeric layer, adsorption of the polymer around the particles of the coated material, and solidification of the microspheres [10, 11].

An alternative in the production of a slow-release fertilizer is to use clay minerals capable of intercalating organic molecules and to perform ionic exchanges. In this study, different percentages of urea were used to be intercalated in expanded vermiculite. For the polymeric coating was used an alginate/collagen solution that was later added into a solution of calcium chloride ($CaCl_2$), formed a spherical structure capable of storing the intercalated urea in expanded vermiculite [7]. In this context, this work has studied the different percentages of urea intercalated in the expanded vermiculite and optimized the different amounts of sodium alginate and collagen in the solution for the encapsulation. Vermiculite was chosen for its potential to be a host for nitrogen sources and is already used in agriculture for its ability to help the absorption of minerals and regulate soil moisture. The vermiculite has the property of reaching an expansive capacity of twenty or even thirty times the normal size original to the basal cleavage plane when submitted to a thermal treatment. Thus, vermiculite becomes an attractive host matrix for the storage of urea as a source of N for crops [12, 13]. In this study, different ratios of urea were used to be intercalated in expanded vermiculite, and for the polymeric coating was used an alginate/collagen matrix to form a spherical structure capable of storing the intercalated urea into expanded vermiculite [14]. In this context, this work has studied different ratios of urea intercalated into the expanded vermiculite and encapsulated these materials into sodium alginate and collagen sphere for potential use as a slow-release fertilizer.

2. Results and Discussion

Expanded Vermiculite Urea intercalation characterization.

The expanded vermiculite (acquired expanded) was kindly supplied by Brasil Minérios for study purposes. The X-ray diffractogram patterns of the samples: expanded vermiculite (EV), urea (U), and the materials intercalated obtained by mechanochemical synthesis, EVUxx% (xx = 10, 20, 30, and 40% wt/wt Urea/EV), are given in Figure 1.

The EV diffractogram pattern (Figure 1b) shows basal peaks (00l), (002), (004), (006), (008), and (0010), which indicates the vermiculite layered structure [15]. This diffractogram shows an intense peak at 6.11°2θ, which is the most characteristic for the Mg-Vermiculite and is associated with the reflection in the plane (002) and is related to two-water layer hydration in the interlayer space of Mg-Vermiculite [16]. This peak corresponding to a basal distance of 14.36 Å, calculated using Bragg's equation ($n\lambda=2.d.\sin\theta$), with the peak of higher order.

The intercalation of urea was confirmed by the first basal reflection (00l) shift to lower angles to the EVU20% sample (Figure 1c); the first peak is centered at 4.93 °2θ and corresponds to a basal distance of 18.25 Å. The diffractions patterns of EVU30% (Figure 1e) and EVU40% (Figure 1f) shown a shift of the first peaks to 4.81 and 5.04 °2θ and correspond to a basal distance of 18.33 and 18.19 Å, respectively [17]. No peak of urea intercalation was observed to EVU10, which is due to the low concentration of urea that did not cause significant changes in the basal distance of the EV or interact only with the surface of EV crystals.

To the samples with 10 and 20 % of intercalated urea, no excess of crystalline urea was observed, indicating that up to 20% of urea results in total intercalation. To EVU30% and EVU40%, an intense a remarkable peak was observed at 22.30 °2θ related to an excess of crystalline urea.

The diffraction angles in Figure 1 for the (002) peak and the correspondent d value are shown in the Table 1, for EV and the urea derivates materials.

The difference in average of approximately 3.8 Å is coherent with the urea intercalation into the vermiculite compared to other examples of urea intercalation in other clay minerals [18].

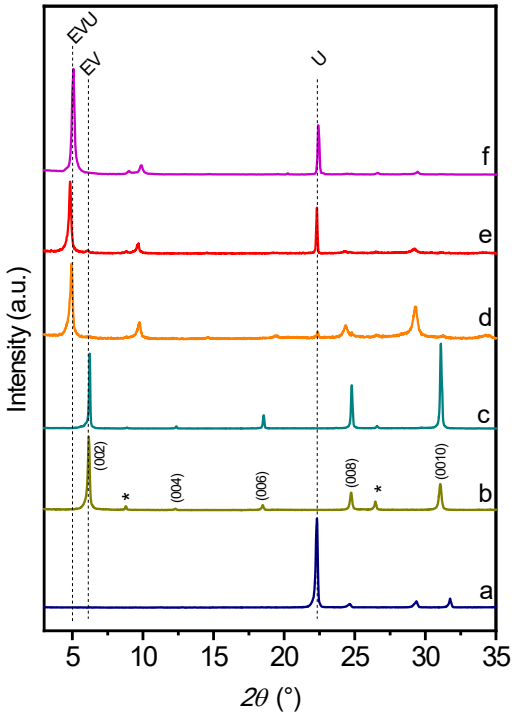

Fig. 1. XRD patterns for: Urea (a), EV (b), EVU10% (c), EVU20% (d), EVU30% (e) and EVU40% (f). (* unidentified impurities).

Table 1. Characterization of the interlayer distance (d(002), Å) of phases EV and their interlayer expansion with urea.

Sample	2θ (002)	d (Å)	Δd*(Å)
EV	6.11	14.36	---
EVU10%	6.18	14.23	-0.13
EVU20%	4.93	17.96	3.60
EVU30%	4.81	18.33	3.97
EVU40%	5.04	18.19	3.83

*Δd is given in relation to EV pure.

The TGA and DSC measurements of the urea, expanded vermiculite, and the EVUxx% samples are shown in Figures 2 and 3, respectively.

The degradation of urea (Figure 2f) starts at a temperature of 122 °C, reaching 463 °C, where the entire sample was consumed. The event of mass loss at the temperature range of 122 to 230 °C corresponds to a loss of 71.55% of mass; this event is related to the release of ammonia and water vapor that acts as an expansion agent [19].

The TGA curve of the expanded vermiculite (Figure 2a), a first degradation step was observed from 30 until 173 °C, which can be explained by the removal of water molecules on the surface of the expanded vermiculite and resulting in the formation of compounds such as forsterite, mullite and alumina [20]. Subsequently, a slight degradation of the sample was observed started at about 704 °C and ending at 978 °C; this event may be related to the dehydroxylation effect of hydroxyl anions in the octahedral layer [21]. The degradation of the expanded vermiculite presented few thermal events because this material already undergoes a thermal heating process to provide its expansion; this also explains why EV lost less weight throughout the analysis.

The EVU10% sample shown four main mass loss events; the first degradation stage occurs at the temperature range between 56.5 and 113 °C, another one from 113 until 434 °C, followed by the loss at 434 – 820 °C and finally a corresponding mass loss of 2.1% in the range of 820 to 978 °C. Another resulting degradation is observed in the thermal region at 615 until 715 °C. However, for EVU samples containing 20% to 40% of urea, a total of three mass loss events occur. It was observed that the total loss of mass increased with the highest percentage of urea content (Table 1). EVU30% and EVU40% curves show an initial degradation temperature at between 100 °C and 260 °C. With the increase in temperature, it was also possible to observe another region of sample degradation that occurred initially at approximately 570 °C and ending at approximately 978 °C, attributed to the exfoliation of the silicate layers that grants the diffusion of the gases generated by the degradation of urea. The TGA results indicate that thermal stability decreased with the increasing percentage of urea, making the aliphatic amide incorporated into the expanded vermiculite a degradation catalyst [22].

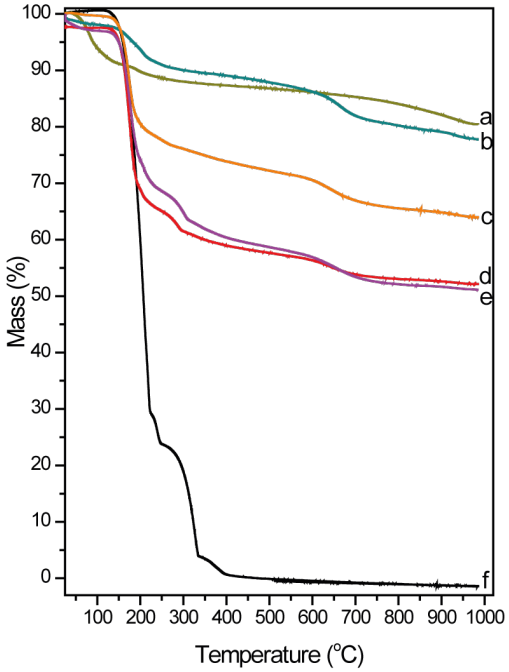

Fig. 2. Thermal analysis (TGA) curves of EV(a), EVU10% (b), EVU20% (c), EVU30% (d), EVU40% (e) and urea (f).

The degradation temperatures of the EV samples, EVU 10%, EVU 20%, EVU 30%, and EVU 40% (wt/wt), are shown in Table 2.

In accordance with the X-ray diffraction analysis, the TGA results revealed that effective intercalations of urea in the interlayer region of expanded vermiculite occurred in the samples EVU10% and EVU20%. The samples of EVU30% and EVU40% also obtained intercalations; however, due to the excess of urea, the TGA curves showed the characteristic urea profile.

According to Figure 3, the first endothermic peak at 134 °C was associated with the removal of free water molecules from the expanded vermiculite, since the samples, even undergoing an expansion process, do not undergo a complete drying treatment, resulting in the water residue on the surface of the layer. The appearance of the second endothermic peak occurs with an increase in temperature of 181 °C, attributed to dehydroxylation caused by the decomposition of some hydrates. Regarding the urea curve represented in black, it is possible to observe a slightly complex decomposition profile, starting a fusion associated with an endothermic peak at 132 °C observed in the DSC. Moreover, there is endothermic

broadband centered at 207 °C, followed by endothermic peaks at 247, 328, and 368 °C. Analyzing the urea curve as a whole was observed that at least four decomposition steps were presented until the complete elimination of the sample [23, 13].

Table 2. Degradation temperatures for urea, EV samples, EVU 10%, EVU 20%, EVU 30% and EVU 40% (wt/wt).

Sample	Events	$T_1 \rightarrow T_2$ (°C)	Mass (%)	Final residue (%)
Urea	release of ammonia and water vapor	122 – 230 230 – 268 268 – 356 356 – 463	71.55 5.44 19.91 3.10	0.00
EV	removal of water molecules	30 – 173 173 – 704	9.26 5.44	80.47
	dehydroxylation effect of hydroxyl anions in the octahedral layer	704 – 978	4.80	
EVU 10%	removal of water molecules and release of ammonia and water vapor	56 – 113 113 – 434 434 – 820	2.00 9.30 8.80	77.83
	exfoliation of the silicate layers that grants the diffusion of the gases generated by the degradation of urea	820 – 978	2.10	
EVU 20%	removal of water molecules and release of ammonia and water vapor	119– 530 530 – 845	27.80 6.53	64.00
	exfoliation of the silicate layers that grants the diffusion of the gases generated by the degradation of urea	845 – 978	1.26	
EVU 30 %	removal of water molecules and release of ammonia and water vapor	123 – 267 267 – 573	33.35 7.40	52.14
	exfoliation of the silicate layers that grants the diffusion of the gases generated by the degradation of urea	573-975	4.60	
EVU 40 %	removal of water molecules and release of ammonia and water vapor	100 – 272 272 – 535	30.00 9.00	51.15
	exfoliation of the silicate layers that grants the diffusion of the gases generated by the degradation of urea	535 – 983	6.85	

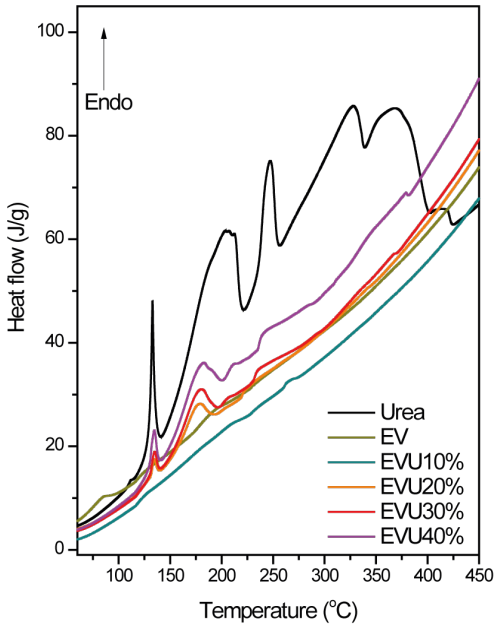

Fig. 3. DSC curves for urea, EV, and EVUxx% samples.

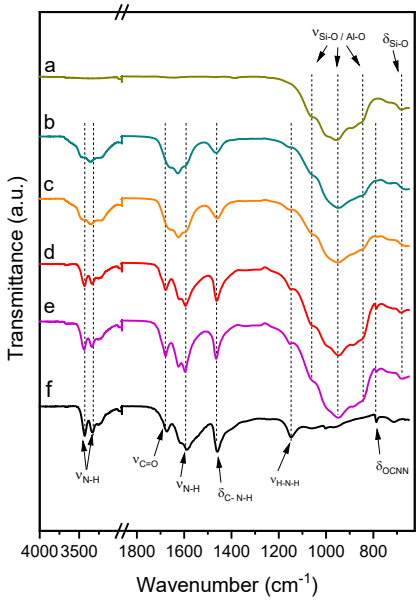

Fig. 4. FTIR spectra of EV(a), EVU10% (b), EVU20% (c), EVU30% (d). EVU40% (e) and urea (f).

Absorption spectroscopy in the infrared region was carried out to identify the existing functional groups and the types of bonding in the structure, including the structural behavior of urea, EV, and EVU 10, 20, 30, and 40%. Figure 4 shows the infrared spectra of the samples mentioned.

Figure 4-a shows the expanded vermiculite spectrum, the peaks at 2981 cm^{-1} (CH_3) and 2888 cm^{-1} (CH_2) correspond to the antisymmetric and symmetrical stretch of the aliphatic C–H bond [20]. At the 1629 cm^{-1} region, weak absorption is identified, representing the O–H vibration of hydration water molecules. Bands with low intensity at 1462–1382 cm^{-1} correspond to the folds of the C–H bond. At 954 cm^{-1} a band with a high-intensity corresponding to the stretching

vibrations of the Si–O of the Si–O–Si silicate bond. In figure 4-a corresponding to the expanded vermiculite's infrared spectrum, there is an absorption band of medium intensity in the region of 1060 and 950 cm^{-1} that indicates the vibrations of the Si–O and Al–O bonds, respectively. At 844 cm^{-1} there is a weak band that is attributed to the stretching of the vibration of the Si–O bond, and a discrete band at 680 cm^{-1} is attributed to the deformation vibration of the Si–O–Si bonds contained in the vermiculite tetrahedral lamellae [24]. For the urea spectrum represented in Figure 4-f, the regions that correspond to the connections of the N–H groups were registered at 3429-3321 cm^{-1}, the C–N bond indicated at 1463 cm^{-1} were analyzed. The peak at 1679 cm^{-1} refers to C=O axial stretch bond, the symmetrical angular strain in the NH or NH_2 plane at 1587 cm^{-1} bend in the C–N–H plane, and NH_2 stretch at 1593 cm^{-1} and 1150 cm^{-1}, respectively [25].

The spectra of urea intercalated with EV containing 10, 20, 30, and 40% (wt/wt), correspond to Figures 4 b-e, respectively. Analyzing the intercalation process in the FTIR analysis, it is possible to verify the appearance of new bands at the regions of 3500 and 3390 cm^{-1}, which indicates that the surface hydroxyls of the EV layered structure are associated with urea molecules. Absorption bands provided by provided by the N–H vibrational stretching of secondary amines in the regions of 3428 and 3320 cm^{-1} and also observed the N–H vibrational stretching in the region close to 1461 cm^{-1} from interactions between urea and EV were also observed [16]. In the 1593 cm^{-1} region, weak absorption was identified, representing symmetrical angular strain in the NH or NH_2 and a short band at 1679 cm^{-1} refers to the axial stretch connection C = O. In the range between 1085 to 954 cm^{-1}, a band with a high-intensity corresponding to the stretching vibrations of the Si–O and the bands of low intensity were attributed to the Si–O–Si vibrations modes. These cited regions indicate that the EV lamellar structures are associated with urea molecules [26].

In figure 4 d-e it is possible to observe that the regions of 1147 cm^{-1} (axial deformation of the N - H), 1679 cm^{-1} (axial deformation of the C = O) and 3428-3320 cm^{-1} (vibrations modes of the group N– H) have the bands of greater intensities in relation to the spectra of figure 4 b-c. This is due to the fact that the EV 30 and 40% samples have higher amounts of urea, making it possible to visualize these regions in the spectrum.

Slow-release essay

In Figure 5 can be observed that the polymeric capsules, as a slow-release fertilizer, have dimensions in the range of 2.0 and 4.8 mm. The granule size has a significant influence on the dilution of the fertilizer. These granules contain adequate dimensions that hinder the rapid dissolution of the material, being dissolved more slowly [27].

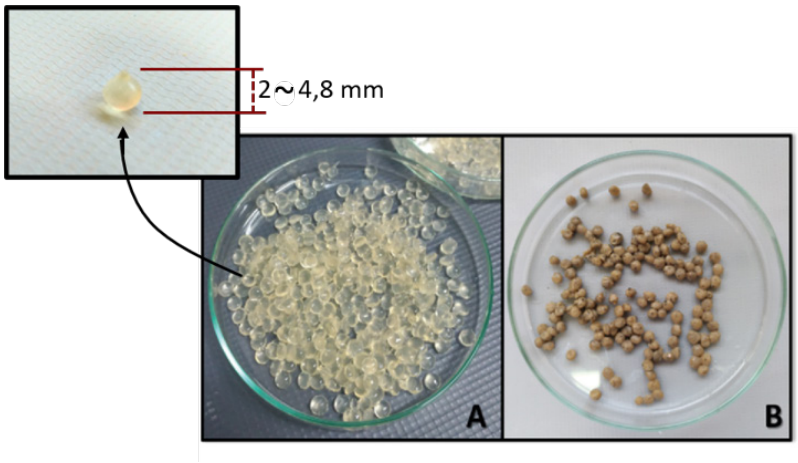

Fig. 5. (A) Alginate/collagen spheres capsules; (B) Alginate/collagen spheres capsules filled with EVU20%.

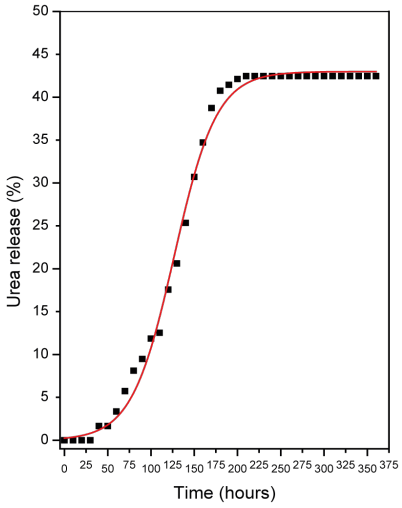

Fig. 6. Urea release curve for the alginate/collagen spherical capsules filled with EV 20% sample.

The slow-release essay showed in Figure 6 was performed on the fertilizer containing the sample EVU20% and encapsulated with 1% sodium alginate and 4% collagen. The essay has shown that the fertilizer can achieve a urea slow-release time in up to 210 hours. A study carried out by Bortoletto-Santos et al., 2016, using the same method with the Ehrlich reagent to quantify the fertilizer produced from the urea coating containing polyurethanes from polyols based on castor oil [28] revealed that the profile of the urea slow-release behavior stabilized over 200 hours. Similar to the fertilizer behavior studied at this work, the slow-release behavior stabilized after 210 hours, with a total amount of urea released by 42%. These studies show that polymeric matrices used as a coating can guarantee a more prolonged urea release [29].

3. Material and Methods

Mechanochemical intercalation of expanded vermiculite (EV) with urea (U)

As previously commented in the text the expanded vermiculite was kindly supplied by Brasil Minérios for study purposes. The preparation of expanded vermiculite (EV) intercalated with urea (U) samples was conducted as follows: 2 g of expanded vermiculite was mixed with 10, 20, 30, or 40 wt.% of urea, for each composition was applied the mechanochemical process, where was performed by mixing the urea and EV in a porcelain mortar. Then the mixture was drily macerated with a porcelain pistil for 30 minutes. The method was adapted from literature [30-32], and the samples were denoted as EVUxx%, where xx = 10, 20, 30, or 40 wt.% of urea intercalated into expanded vermiculite.

Formation of polymeric spherical capsules

After obtaining the EVUxx% materials, the next step consisted of preparing a polymeric coating matrix, where added in a beaker containing 100 mL of distilled water, 1% (wt/vol) sodium alginate, and 4% (wt/vol) hydrolyzed collagen. This solution remained under magnetic stirring for 24 h at 50 °C. Then it was dripped with a peristaltic pump on a solution containing 100 mL of 3% (wt/vol) $CaCl_2$ [33]. It was necessary to wait approximately 6 hours for the complete reticulation of the spherical capsules. The capsules were stored in a petri dish and dried at room temperature [34].

The same process was employed for the preparation of the spherical capsules added with the EVU20% materials. For this, the intercalated material was initially dispersed in the solution containing sodium alginate and collagen, and the next steps followed the procedure described above. The process steps are shown in Figure 7.

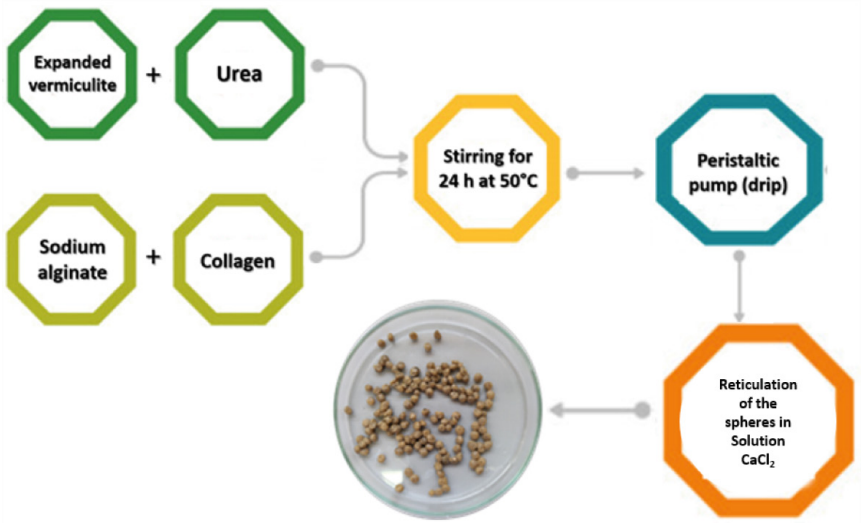

Fig. 7. Schematic representation of the polymeric spherical capsules' synthesis containing the EVU20% materials.

Release assay

The spherical capsules synthesized were subjected to a urea release assay, where the process consisted of weighing 1 g of the spheres and adding them in a 150 ml beaker containing 100 ml of water. The method for quantifying the concentration of released urea was adapted from With et al. [35] and analyzed by UV-Vis spectrometry. Thus, 1 g of fertilizer sphere containing 20% urea was weighed and mixed with 2.5 ml of a solution containing 10% trichloroacetic acid and 0.500 ml of Ehrlich reagent. The system was monitored every 10 hours for 360 hours [36].

Measurement and characterization

The samples and reagents were characterized by X-ray powder diffraction (XRD) obtained from a Bruker X-ray diffractometer, model D2Phaser, Cu K_a radiation (λ = 1.5418 Å), 40 kV potential, 30 mA current, range between 3° and 35° (2θ) and increment of 0.05 °/s.

The thermogravimetric analysis measurements were performed with TGA/DSC Perkin Elmer STA 6000 under an air atmosphere, between temperatures of 25 to 1,000 ºC and heating rate of 10 ºC/min, using platinum crucible containing approximately 4.0 mg of sample.

The infrared spectra of products were obtained by the Fourier transform spectrometer (FTIR) model 6000, Perkin Elmer with Attenuated Total Reflectance (ATR) module FTIR Frontier region 4000—650 cm^{-1}, resolution 4 cm^{-1}.

The analysis of the UV-Vis was measured at Ocean Optics spectrophotometer model LS^{-1}, equipped with support for solids and tungsten lamp, and the analysis was collected between 400 and 500 nm.

4. Conclusions

The results indicated that the mechanochemical method intercalated the urea into the interlayer space of the expanded vermiculite. This fact was observed principally in the XRD results, where XRD analysis has shown the EVU20% sample was the most appropriate percentage of urea because the sample obtained the highest percentage of intercalated urea without the presence of crystallized urea after the mechanochemical process.

The release test proved that it was possible to produce spherical capsules with a size between 2.0 and 4.8 mm for the encapsulation of EVU20% sample, and this polymeric matrix had promoted a diffusional barrier to the urea release. The release test showed durability of approximately 210 hours and a total amount of 42% urea released by the system. In this way, the spherical capsules produced between the polymeric matrix and the vermiculite intercalated with urea have the potential to act as a slow-release fertilizer as a source of nitrogen for food crops.

Acknowledgments

This study was supported by the Conselho Nacional de Desenvolvimento Científico e Tecnológico (CNPq) [grant number 455906/2014-9]. This study was financed in part by the Coordenação de Aperfeiçoamento de Pessoal de Nível Superior - Brasil (CAPES) - Finance Code 001.

Author Contributions

D. S. Oliveira, S. Jaerger and R. Marangoni contributed in investigation, conceptualization, methodology, synthesis, formal analysis, validation and writing. Specifically, D. S. Oliveira and R. Marangoni through the TEQMA laboratory contributed in funding acquisition, resources, supervision, review and editing of the manuscript.

References and Notes

[1] Zulfiqar, F.; Navarro, M.; Ashraf, M.; Akram, N. A. *J. Plant Science*, **2019**, *289*, 110. [Crossref]

[2] Maqbool, Q.; Sidorowirz, A.; Nazar, M.; Jabeen, N.; Anwaar, S.; Ahmad, I. *J. Mater. Today Commun.* **2019**, *20*, 100544. [Crossref]

[3] Hai-yan, W.; Zhi-peng, X.; Lei, Z.; Qiu-yuan, L.; Zhen-Zhen, Z.; Yan, J.; Ya-Jie, H.; Jin-yan, Z.; Pei-yuan, C.; Qi-gen, D.; Hong-cheng, Z. *J. Integr. Agric.* **2018**, *17*, 2234. [Crossref]

[4] Frazão, J. J.; Benites, V. M.; Ribeiro, J. V. S.; Pierobon, V. M.; Lavres. *J. Geoderma* **2019**, *337*, 593. [Crossref]

[5] Elhassani, C. E.; Essamlali, Y.; Aqlil, M.; Nzenguet, A. M.; Ganetri, I.; Zahouily, M. *Environ. Technol. Innovation.* **2019**, *15*, 100403. [Crossref]

[6] Kenawy, E.; Azaam, M. M.; El-nshar, E. M. *Arabian J. Chem.* **2019**, *12*, 856. [Crossref]

[7] Hermida, L.; Agustian, J. *Environ. Technol. Innovation.* **2019**, *13*, 121. [Crossref]

[8] Madusanka, N.; Sandaruwan, C.; Kottegola, N.; Sirisena, D.; Munaweer, I.; Alwis, A.; Karunartne, V.; Amaratunga, G. A. J. *Appl. Clay Sci.* **2017**, *150*, 30. [Crossref]

[9] Rudmin, M.; Banerjee, S.; Yakich, T.; Tabakaev, R.; Ibraeva, K.; Buyakov, A.; Soktoev, B.; Ruban, A. *Appl. Clay Sci.* **2020**, 196, 105775. [Crossref]

[10] Costa, J. C. M.; Santos, G. L. A.; Araújo, E. S.; Alves, E. S. *Braz. J. Develop.* **2020**, *6*, 93382. [Crossref]

[11] Lima, A. M. F.; Andreani, L.; Soldi, V. *Quim. Nova* **2007**, *30*, 837. [Crossref]

[12] Marcos, C.; Rodrígues, I. *Appl. Clay Sci.* **2010**, *48*, 498. [Crossref]

[13] Fan, E.; Hu, F.; Miao, W.; Xu, H.; Shao, G.; Liu, W.; Li, M.; Wang, H.; Lu, H.; Zhang, R. *Appl. Clay Sci.* **2020**, *197*, 105789. [Crossref]

[14] Pilipenko, N.; Gonçalves, O. H.; Bona, E.; Fernandes, I. P.; Pinto, J. A.; Sorita, G. D.; Leimann, F. V.; Barreiro, M. F. *Carbohydr. Polym.* **2019**, *223*, 115035. [Crossref]

[15] Wiewióra, A.; Pérez-Rodríguez, J. L.; Perez-Maqueda, L. A.; Drapala, J. *Appl. Clay Sci.* **2003**, *24*, 58. [Crossref]

[16] Fu, Z.; Liu, T.; Kong, X.; Liu, Y.; Xu, J.; Zhang, B.; Chen, H.; Chen, Z. *Mater. Lett.* **2018**, *238*, 178. [Crossref]

[17] Lacerda, J. G. P.; Candeia, R. A.; Sales, L. L. M.; Araújo, A. S.; Cunha, A. F. P. Wanderley, A. F.; Campos, A. F. *J. Therm. Anal. Colorim.* **2019**, *137*, 2052. [Crossref]

[18] Gardolinski, J. E.; Wypych, F. *Quim. Nova*. **2001**, *24*, 767. [Crossref]

[19] Almeida, J. C.; Barroa, A.; Mazali, I. O.; Ferreira, M. *Appl. Surf. Sci.* **2020**, *507*, 144972. [Crossref]

[20] Valdrè, G.; Malferrari, D.; Marchetti, D.; Brigatti, M. F. *Appl. Clay Sci.* **2007**, *35*, 84. [Crossref]

[21] Liang, Y.; Yu J.; Feng, Z.; Ai, P. *Constr. Buil. Mater.* **2013**, *48*, 1119. [Crossref]

[22] Júnior, R. M. S.; Oliveira, T. A.; Araque, L. M.; Alves, T. S.; Carvalho, L. H.; Barbosa, R. *J. Mater. Res. Technol.* **2019**, *8*, 3243. [Crossref]

[23] Muiambo, H. F.; Focke, W.W.; Atanasova, M.; Benhamida, A. *Appl. Clay Sci.* **2015**, *105*, 20. [Crossref]

[24] Feng, J.; Liu, M.; Fu, L.; Shaojian, M.; Yang, J.; Mo, Y.; Su, X. *Ceram. Int.* **2020**, *46*, 6417. [Crossref]

[25] Xiaoyu, N.; Yuejin, W.; Zhengyan, W.; Lin W.; Guannan, Q.; Lixiang, Y. *Bioprocess Biosyst. Eng.* **2013**, *115*, 282. [Crossref]

[26] Zhao, M.; Zhaobin, T.; Liu, P. J. *Hazard. Mater.* **2008**, *158*, 51. [Crossref]

[27] Liu, Y.; Gao, C.; Wang, Y.; He, L.; Lu, H.; Yang, S. *J. Cleaner Prod.* **2020**, *254*, 120111. [Crossref]

[28] Bortoletto-Santos R.; Ribeiro, C.; Polito, W. L. *J. Appl. Polym. Sci.* **2016**, *133*, 8. [Crossref]

[29] Silva, E. F.; Escanio, C. A.; Oliveira, M. A.; Bezerra, A. C. S.; Machado, A. R. T. *Rev. Mater.* **2019**, *24*, 3. [Crossref]

[30] Al-Rawajfeh, A. E.; AlShamaileh, E. M.; Alrbaihat, M. R. *J. Ind. Eng. Chem.*, **2019**, *73*, 343. [Crossref]

[31] Teodoro, L.; Parabocz, C. R. B.; Rocha, R. D. C. *Rev. Mater.* **2020**, *25*, 8. [Crossref]

[32] Borges, R.; Brunatto S. F.; Leitão, A. A.; Carvalho, G. S. G.; Wypych, F. *Clay Miner.* **2015**, *50*, 162. [Crossref]

[33] Surya, R.; Mullassery, M. D.; Fernandez, N. B.; Thomas, D. *J. Sci.: Adv. Mater. Devices*. **2019**, *4*, 441. [Crossref]

[34] Luo, W.; Huang, Q.; Antwi, Q.; Antwi, P.; Guo, B.; Sasaki, K. *J. Colloid Interface Sci.* **2020**, *560*, 348. [Crossref]

[35] With, k.; Petersen, T. D.; Petersen, B. *J. Clin. Pathol.* **1961**, *14*, 204. [Crossref]

[36] Matos, M.; Mattos, B. D.; Tardy, B. L.; Rojas, O. J.; Magalhães, W. L. E. *ACS Sustainable Chem. Eng.* **2018**, *6*, 2723. [Crossref]

How to cite this article

De Oliveira, D. S.; Jaerger. S.; Marangoni, R. *Orbital: Electron. J. Chem.* **2021**, *13*, 124. http://dx.doi.org/10.17807/orbital.v12i2.1488